Star polymers rupture induced by constant forces

N. A. García, M. Febbo, D. A. Vega, and A. Milchev

Citation: The Journal of Chemical Physics **141**, 164907 (2014); doi: 10.1063/1.4899048
View online: http://dx.doi.org/10.1063/1.4899048
View Table of Contents: http://scitation.aip.org/content/aip/journal/jcp/141/16?ver=pdfcov
Published by the AIP Publishing

Star polymers rupture induced by constant forces

N. A. García,[1] M. Febbo,[1,a)] D. A. Vega,[1] and A. Milchev[2]
[1]*Instituto de Física del Sur (IFISUR-CONICET) and Departamento de Física, Universidad Nacional del Sur, Avda. Alem 1253, 8000 Bahía Blanca, Argentina*
[2]*Bulgarian Academy of Sciences, Institute of Physical Chemistry, 1113 Sofia, G. Bonchev Str. Bl.11, Bulgaria*

(Received 4 August 2014; accepted 10 October 2014; published online 28 October 2014)

In this work, we study the breakage process of an unknotted three-arm star-shaped polymer when it is pulled from its free ends by a constant force. The star polymer configuration is described through an array of monomers coupled by anharmonic bonds, while the rupture process is tracked in three-dimensional space by means of Langevin Molecular Dynamics simulations. The interaction between monomers is described by a Morse potential, while a Weeks-Chandler-Anderson energetic contribution accounts for the excluded volume interaction. We explore the effect of the molecular architecture on the distributions of rupture times over a broad interval of pulling forces and star configurations. It was found that the rupture time distribution of the individual star arms is strongly affected by the star configuration imposed by the pulling forces and the length of the arms. We also observed that for large pulling forces the rupture time distributions resemble the dominant features observed for linear polymer chains. The model introduced here provides the basic ingredients to describe the effects of tensile forces on stress-induced degradation of branched macromolecules and polymer networks.
 [http://dx.doi.org/10.1063/1.4899048]

I. INTRODUCTION

The phenomenon of thermo-mechanical degradation in macromolecular systems is an ubiquitous phenomenon of immense basic and technological importance. Examples where this phenomenon plays a key role include polymer mastication in tire manufacturing, micromanipulation of synthetic and natural biopolymers, polymer recycling and the mechanical stability of engineering polymers. The understanding of the phenomenon of thermo-mechanical degradation raises also a number of important questions from the point of view of fundamental science. One of the key questions concerns, *inter alia*, the effect of macromolecule architecture in branched polymers on their stability when these polymers are subjected to tensile forces. Clearly, these studies are prompted by the need to elucidate the relationship between polymer architecture and tensile stability in view of the massive involvement novel synthesized soft matter materials in emerging technologies.

Apparently, an essential precondition in answering the aforementioned problems implies the clarification of the thermo-mechanical stability of linear macromolecules. A step towards the understanding of the dynamics of polymer thermo-mechanical degradation was recently done by Paturej *et al.*,[1,2] who used Molecular Dynamics (MD) modeling to study the mechanisms of polymer chain scission for linear polymers subjected to a constant tension. In this case it was found that the average mean life time $\langle\tau\rangle$ for a chain of length N becomes progressively independent of the number of bonds as the pulling force increases and that $\langle\tau\rangle$ depends on chain length like a power law ($\langle\tau\rangle \sim N^{-\beta}$), with an exponent within the interval $0 < \beta < 1$. The results also indicate that as the applied force is increased the process of chain scission involves an increasing degree of cooperativity during the chain breakage.

The main motivation of the present work is to understand the breakage process under the action of constant external tensile forces for star-shaped polymers and to explore the changes in the Mean First Breakage Time (MFBT) due to branching. Branching appears not only in a wide diversity of model polymers (pompom's, H's, comb's, etc.), but also in commercial branched polymers such as low density polyethylene or synthetic and natural rubbers.[3–7]

The presence of branching deeply affects the dynamics of polymers and also may introduce a geometrical effect in the distribution of line tension along the different arms in the branched structure. Moreover, it has been found experimentally by Matyjaszewski *et al.*[8–10] recently, that the tension in covalent bonds may reach orders of magnitude higher values upon adsorption of brushlike macromolecules onto a substrate. Meanwhile, in several works Panyukov and co-workers[11,12] predicted and theoretically described the effect of tension amplification in branched macromolecules. These analytical considerations have been found to comply also with the results of MD computer experiments.[13,14] As the polymer architecture with the lowest degree of complexity that introduces the effect of branching is the three-arm star-shaped polymer, here we focus our study in this system. However, the main conclusions drown here can be easily extrapolated to polymers with more complex branched architectures.

II. MODEL

In order to analyze the MFBT of the star polymer under tension, we consider a coarse-grained model where the

a)Author to whom correspondence should be addressed. Electronic mail: mfebbo@uns.edu.ar. Tel.: (+54-291) 4595141. Fax: (+54-291) 4595141.

polymer is described through an array of beads connected by appropriated bonds (see a schematic representation in Fig. 1(a)). The physical description of the star consists of an array of three arms of equal length, each one having N monomers, plus a tri-functional monomer connecting the different branches. Then, the star polymer is constituted by a total of $N_t = 3N + 1$ monomers.

Successive beads are connected by bonds, whereby each bond of length b is described by a Morse potential, $U^M(r) = D\{1 - \exp[-a(r-b)]\}^2$, where a determines the bond elasticity ($a = 1$ in our case) and D is the dissociation constant, which measures the dissociation energy of a given bond in units of k_bT, where k_b is the Boltzmann constant and T is the temperature.[15] The total potential energy is

$$V^M(\{\mathbf{q}_i\}) = \sum_{i=0,s=1}^{N,3} U^M\left(\mathbf{q}_i^s - \mathbf{q}_{i-1}^s\right) - f_s \mathbf{q}_N^s, \qquad (1)$$

where subscript s denotes number of the arm of the star polymer. Additionally, we set $\mathbf{q}_0^s$ as the center monomer. Upon change of variables, $\mathbf{y}_i^s = \mathbf{q}_i^s - \mathbf{q}_{i-1}^s$, it is possible to write

$$V^M(\{\mathbf{q}_i\}) = \sum_{n=1,s=1}^{N,3} \left[U^M\left(\mathbf{y}_n^s\right) - f_s \mathbf{y}_N^s\right] = \sum_{n=1,s=1}^{N,3} U\left(\mathbf{y}_n^s\right) \qquad (2)$$

so the combined one-bond potential is $U(y) = D\{1 - \exp[-ay]\}^2 - fy$ (see Fig. 1(b)). The position of the metastable minimum y_- and of the maximum y_+ are given by

$$y_{-,+} = \frac{1}{a} \ln\left[\frac{2}{1 \pm \sqrt{1-\tilde{f}}}\right], \qquad (3)$$

where the dimensionless force is $\tilde{f} = 2f/aD$. The activation energy (barrier height) is given by

$$\Delta E_b = U(y_+) - U(y_-) = D\left\{\sqrt{1-\tilde{f}} + \frac{\tilde{f}}{2} \ln\left[\frac{1-\sqrt{1-\tilde{f}}}{1+\sqrt{1-\tilde{f}}}\right]\right\}. \qquad (4)$$

Evidently, ΔE_b decreases with $\tilde{f}$. In order to allow the excluded volume interaction, which is not possible to achieve only with V^M due to its weak repulsion over short distances, we take the bond potential as a sum of V^M and the Weeks-Chandler-Anderson (WCA) potential, given by the following expression:

$$V^{WCA}(r) = \begin{cases} 4\epsilon\left[\left(\frac{\sigma}{r}\right)^{12} - \left(\frac{\sigma}{r}\right)^{6} + \frac{1}{4}\right], & \text{if } r \le b \\ 0, & \text{else,} \end{cases}$$

where ϵ and σ are assumed to be 1. The parameter σ fixes the length scale of the equilibrium bond length $b = 2^{1/6}\sigma \approx 1.12$.

III. SIMULATION RESULTS

The Brownian motion of the different bounded beads is described through a Langevin dynamics, where the position of n-bead in the star $\mathbf{q}_n$ is tracked in time. Here we consider that the monomer located at the free-end of each arm is subjected to a external pulling force $\mathbf{f}_i$ ($i = 1, 2, 3$) whose values ensure that the center of mass of the star is under a net zero force. Because of the geometric distribution of the proposed star chain, we will consider $f = f_1 = f_2; f_3 = 2f_1 \sin\theta$ (see Fig. 1(a)).

In order to track the dynamics of chain scission, here we follow the method described in Ref. 1. Following this approach, the stochastic initial condition for the star was obtained running the Langevin dynamics during 5×10^4 time steps at low temperatures. The time step used was

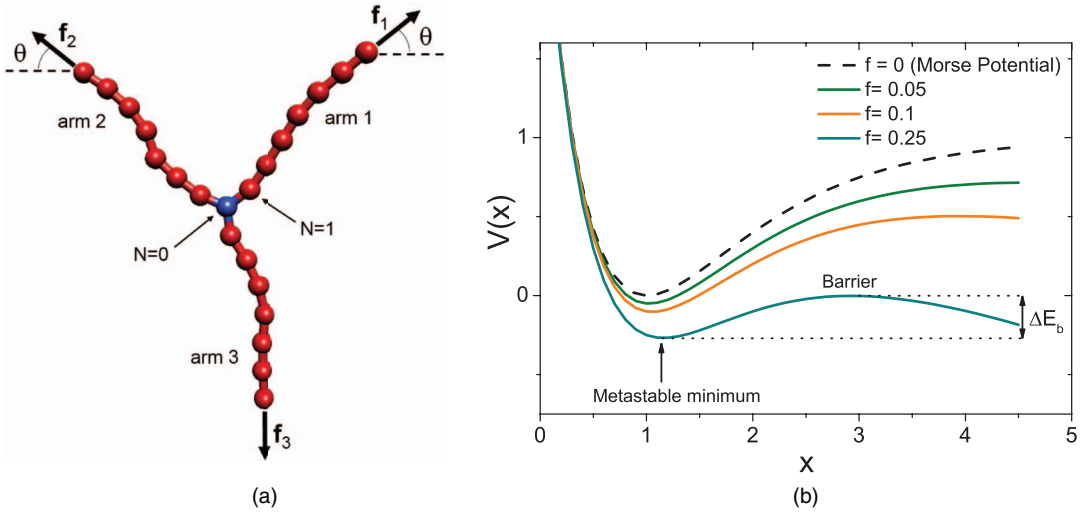

FIG. 1. (a) Schematic representation of the star polymer system under study. In this scheme, the blue bead marks the position of the branching point. Here $\mathbf{f}_3$ points along the vertical axis, while the direction of $\mathbf{f}_1$ and $\mathbf{f}_2$ is imposed by the condition that ensure the dynamic equilibrium of the center of mass ($\Sigma_{i=1,3}\mathbf{f}_i = \mathbf{0}$). Note that $\mathbf{f}_1$ and $\mathbf{f}_2$ make an angle of θ with the horizontal. (b) Modified Morse Potential. The presence of a pulling force in the Morse potential ($f = 0$) gives rise to a metastable minimum and a activation energy E_b; observe that the barrier height ΔE_b declines with growing force f.

$dt = 0.002$. This process prevents chain scission during the thermalization within the range of pulling forces explored here. Once the initial condition was obtained, the time evolution of the system was analyzed at a fixed temperature of $T = 0.053$ with a friction coefficient of $\gamma = 0.2$. The simulations were computed in three-dimensional space. The trajectories explored by the individual beads during the time elapsed before scission is recorded in order to obtain their time-average mean displacements. Every scission process was done 50 000 times to obtain an average value. We use a critical bond extension, $r_h = 5b$ which is defined as a threshold to a broken state.[15]

IV. NUMERICAL COMPARISON AND DISCUSSION

In Secs. IV A–IV D, we analyze the distribution of Mean First Breakage Time $\langle\tau\rangle$ as a function of the total number of monomers N_t for different values of the pulling force together with the most salient properties of the bond rupture processes. As we show below the scission process is controlled by three variables: chain length, magnitude of the pulling force, and star configuration.

A. Probability density functions

Previously, it has been found that the bonds which have a larger mobility or excursions in space break more easily than more slower bonds.[1] In order to explore qualitatively the effect of the local mobility on the scission process, here we analyze the distribution of star configurations with the aid of the Probability Density Functions (PDF) $P(\mathbf{q}_n)$. Here the PDF is a measure of the average excursions of the star with regard to the center of mass-made by the different monomers during the time span up to a chain scission event. The PDF, represented through three dimensional density color plots in 3D space, are obtained through a time average. The results for $P(\mathbf{q}_n)$ for star configurations with three different angles $\theta = 10^\circ, 30^\circ, 60^\circ$ and two different forces $f_1 = 0.1$ and $f_1 = 0.2$ can be observed in Fig. 2.

As a general feature, it is possible to clearly observe the stretching process that suffers the star polymer as consequence of the increasing pulling forces. This process can be seen as a slimming of the $P(\mathbf{q}_n)$ perpendicular to the direction of the line connecting the star free ends with the branching point and at the same time a stretching of each arm in the direction of the force. For non-symmetric distributions of the pulling forces ($\theta \neq 30^\circ$), it also results in a symmetry breaking of the distribution $P(\mathbf{q}_n)$ along the third arm. For example, note that due to the different pulling force that experiences this arm, for large angles ($\theta \sim 90^\circ$) it has to support about twice the pulling force of the other two arms. Consequently, as compared with their partners, the third arm suffers a stronger stretching.

Then, regardless of the value of the angle, large pulling forces prevent the system to have large excursions in a direction perpendicular to the line connecting the free ends with the branching point of the star. Consequently, one can expect that this constraint increases the probability of rupture at the end points of any arm, a result previously observed for linear chains.[1] A different situation is observed at low angles since in this case the third arm is subjected to an extremely low force. For low applied pulling forces it can be seen that the system makes larger excursions. Then, one may expect that the polymer is more likely to break in the neighborhood of the cross-linker point. However, as we show below, although the PDF provides useful information about the star configuration during the previous instances to chain scission, it is not possible from these distribution maps to predict which particular arm is actually going to break. We must recall that the scission process is governed not only by the local mobility of the different beads, but also by a complex interplay between the distribution of stress along the different arms and the inertial effects introduced by the branching point.

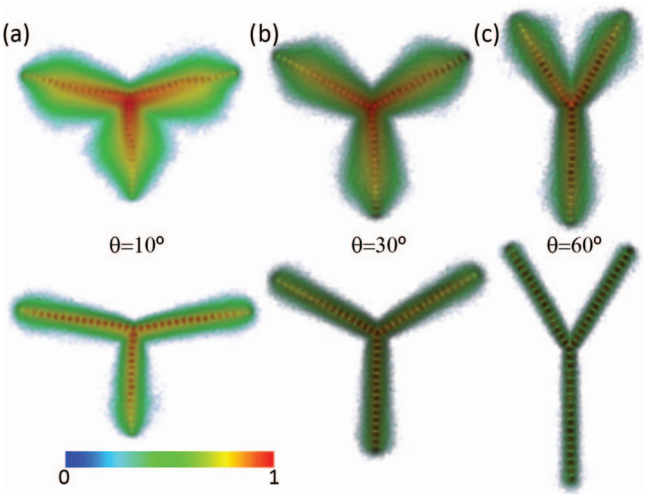

FIG. 2. (a)–(c) Probability density distribution $P(\mathbf{q}_n)$ for a system with $N_t = 49$ particles (arm length involves 16 bonds) and different star configurations and stretching forces: $f = 0.1$ (upper panels) and $f = 0.2$ (bottom panels). Here $P(\mathbf{q}_n)$ is represented through the color map shown at the bottom left. Note that irrespectively of the dominant orientation of the star polymer, the arms suffer an increasing deformation as the magnitude of the force increases.

B. Chain length dependence of the MFBT $\langle\tau\rangle$

Lets consider the dependence of $\langle\tau\rangle$ as a function of N_t for values of pulling forces within the range $0.1 \leq f \leq 0.2$. Figure 3 show the MFBT $\langle\tau\rangle$ of a star polymer for different pulling forces and star configurations. Here, $\langle\tau\rangle$ denotes the average star rupture time, independently of which bond breaks first. As a general aspect, we can observe in these figures that $\langle\tau\rangle$ depends strongly on both, chain length and angle.

For large N_t ($N_t \geq 100$), it can be observed that $\langle\tau\rangle$ is relatively insensitive to the star configuration and that $\langle\tau\rangle$ follows a power law: $\langle\tau\rangle \propto N^{-\beta}$. As shown in Fig. 4, the exponent in the power law β decreases with the applied pulling force regardless of the angle θ and it is only slightly dependent on the star configuration. We also note that the exponents are similar to those found for linear polymers under similar conditions, where it was found that the exponent β changes within the range $0 < \beta < 1$.[1] In agreement also with the results for linear chains, at intermediate chain lengths $20 \leq N_t \leq 100$ the MFBT also decreases as the chain length increases. However, in this region $\langle\tau\rangle$ does not follow a power law but

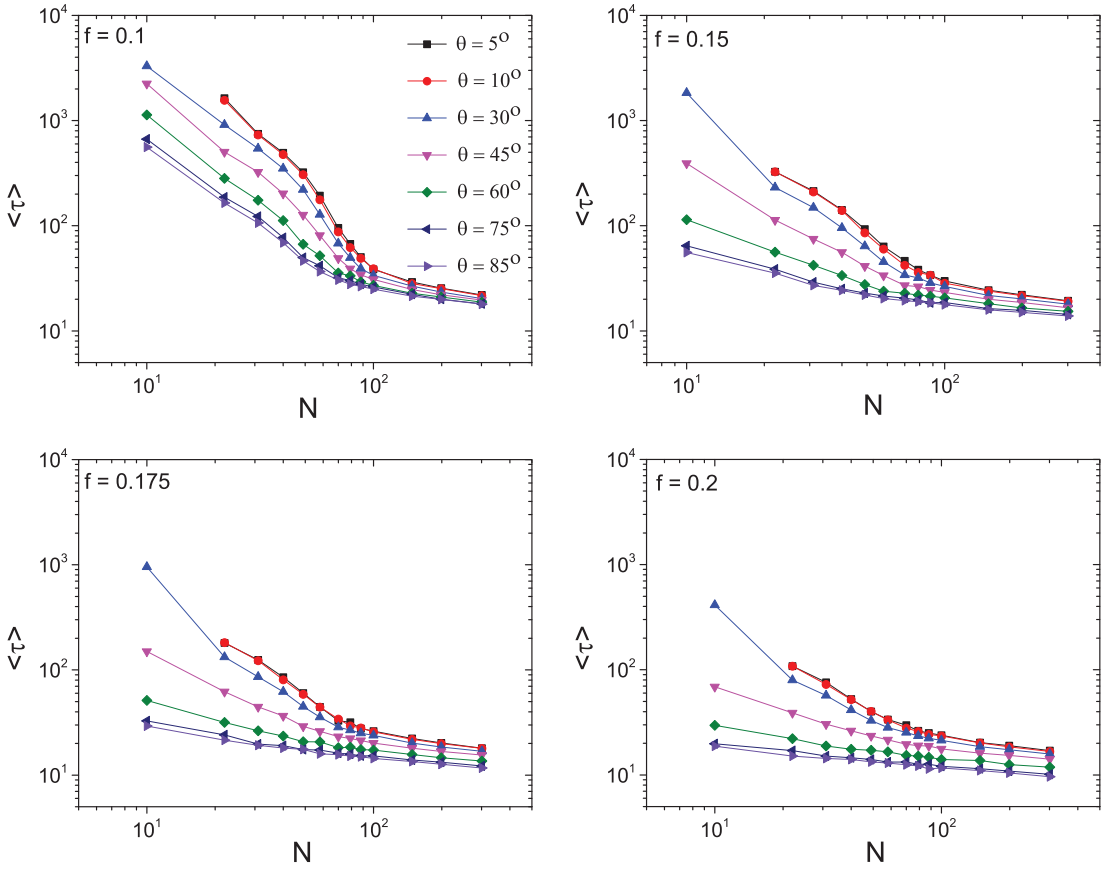

FIG. 3. Mean first breakage time $\langle\tau\rangle$ vs. the total number of monomers N_t for different angles and stretching forces. Symbols and values of the stretching forces indicated in the figure.

a more complex behavior. Observe also that within this range of chain lengths, $\langle\tau\rangle$ is strongly dependant on θ and any increment in the force shifts the distributions to lower times. Note also that for the shorter chain lengths explored here ($N_t \leq 20$), the MFBT also changes qualitatively its dependence with N_t.

The dependence of $\langle\tau\rangle$ with the distribution of applied forces is more clearly emphasized in Fig. 5. It is possible to observe a decrement of $\langle\tau\rangle$ as the angle increases. However, this tendency is not so marked as we increase the magnitude of the applied force. In addition, the curves change in concavity for an angle of $\theta = 30$ (inflexion point) which corresponds to the symmetric star configuration. As soon as the angle increases, all curves become insensitive to the star configuration, situation that resembles the results obtained when the chain length is varied.

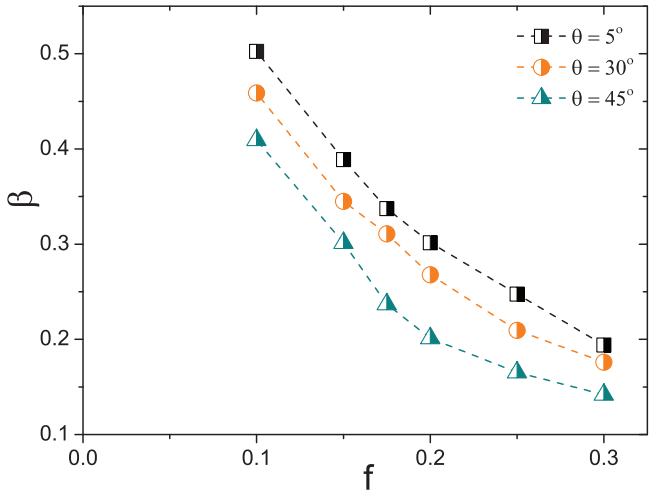

FIG. 4. Power law exponent β for the mean first breakage time as a function of the pulling force and θ: $\langle\tau\rangle \propto N^{-\beta}$.

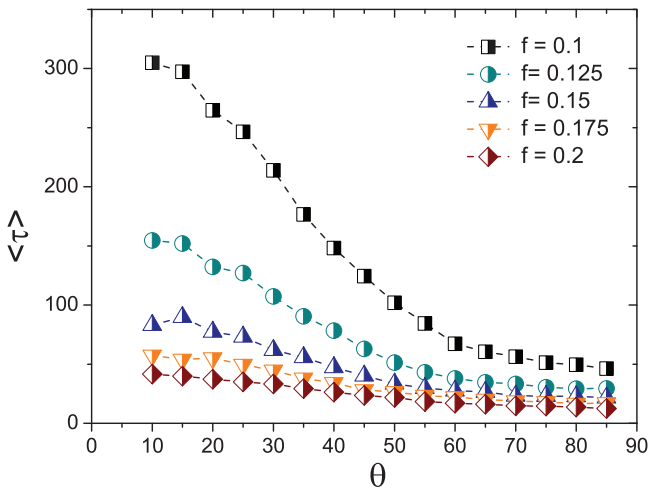

FIG. 5. Mean first breakage time $\langle\tau\rangle$ vs. θ for a set of different tensile forces (here $N_t = 49$).

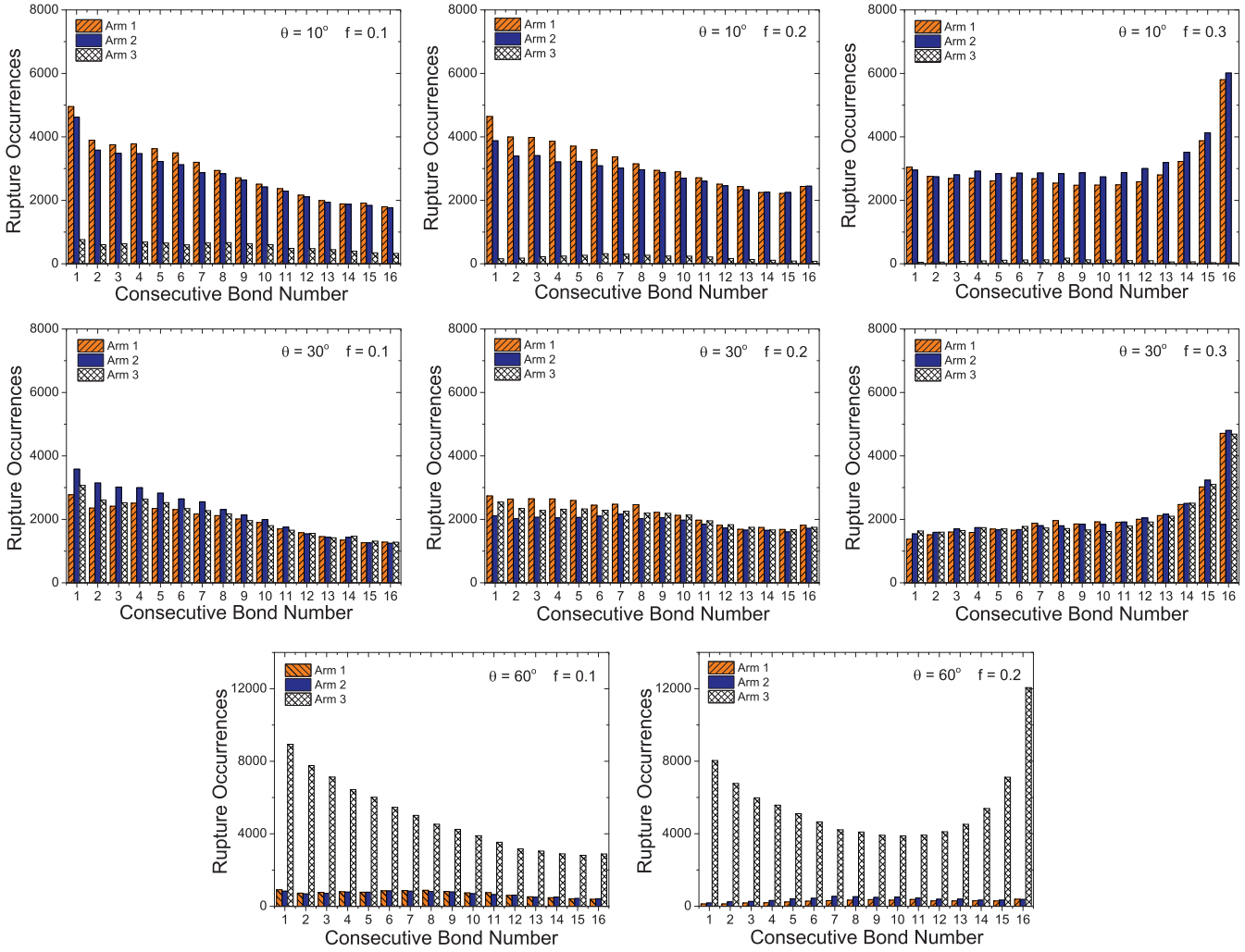

FIG. 6. Bond rupture occurrence distribution for a star chain composed of $N_t = 49$ particles for different values of f and θ.

C. Angle dependence of the MFBT

Although it was observed that $\langle \tau \rangle$ is affected by the star configuration, it is useful to analyze the distribution of rupture times along the different branches in order to identify the regions more sensitive to chain scission.

Figure 6 shows the histograms with the distribution of MFBT along the bonds constituting the different branches. For labeling the bonds, we assume that the bead 0 identifies the branching point. The other bonds are labeled in increasing order as they get further away from the branching point (see the scheme of Figure 1). For simplicity, here we focus the attention in star shaped polymers with $N_t = 49$, which implied arms with a size $N = 16$. Therefore, for this configuration the bond 1 links the branching point bead to its first neighbors along each star arm, whereas the bond 16 provides the connectivity to the last bead of each arm. In this figure, it can be observed that due to the symmetry in the applied pulling forces, the histograms corresponding to the first and second branches present similar features ($f_1 = f_2$), while the histograms corresponding to the third star arm may be different, depending upon the star configuration.

Note in Figure 6 that, independently of the values of the pulling force, for small values of θ there is a large rupture probability for the bonds located in the first and second arms as compared with the corresponding to the third arm. It can be expected that for low angles the star has similar distribution of breakages as a linear chain with $2N + 1$ beads (see Sec. IV D) regardless the existence of the branching point and the third arm, which has a poor contribution in the rupture process. This is attributable to the relatively low value of the pulling force $f_3 = 2f_1 \sin(10) \approx 0.35 f_1$ acting along the third arm. As the force increases, the maximum of the distribution shifts from the bond connecting the branching point (bond #1) to the bond located at the free end (bond #16), indicating that a large pulling force tends to break the bonds at the end of each arm. Additionally, the rupture probability of the third arm decreases as the force increases, being negligible for the largest applied forces. Note also that the maximum of the distribution of breakages in the third arm displaces to the middle bond since this branch behaves as a linear chain under small pulling forces. Observe in Figure 6 that for $\theta = 30^\circ$, the results evidence the expected symmetry of the three arms in the distribution of breakages. Similar to single linear chains, upon increasing the pulling force, the bonds located in the neighborhood of the free ends increase the probability of scission.[1]

Increasing the angle to 60°, the distribution of breakages differs very markedly with respect to the previous cases,

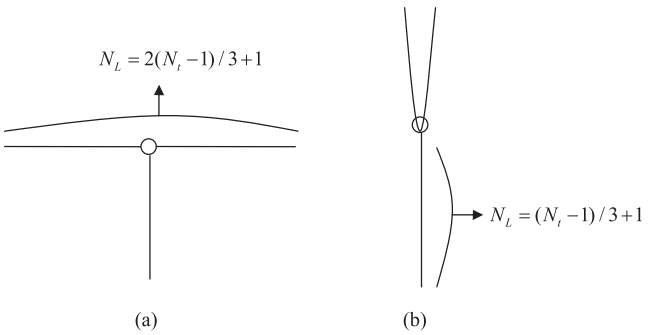

FIG. 7. Schematic diagram to emphasize the comparison between the behavior of linear and star shaped polymers in the small and large angle limits. (a) Low angle limit. (b) Large angle limit.

revealing the important angle dependence of the breakage process. Moreover, it is possible to observe an important scission process in the third arm for low and intermediate forces. For small forces, the rupture process occurs mainly in the neighborhood of the branching point, while for intermediate values of the pulling force ($f = 0.2$) the distribution of breaking times presents a minimum at the middle of the arm, with the bonds located in the neighborhood of the free ends contributing similar to those in the neighborhood of the branching point, in agreement also with the results for linear chains.[1]

Summarizing, it can be claimed that for low angles the rupture process takes place mainly in the first and second arms, while for large angles the contribution of the third arm prevails. One remarkable feature for this system is that star configuration may increase the chance of chain scission up to one order of magnitude due to the purely geometric effects associated with the distribution of pulling forces.

D. Comparison between linear and star polymer of the same length

Here, we wish to compare quantitatively the MFBT of a linear and star chain with equivalent number of monomers (see the scheme of Fig. 7). In order to understand the correlation between linear polymers and stars, we performed different simulations under two limit conditions (small and large angles). For a meaningful comparison, we considered the scission process of linear chains with N_L monomers ($N_L = 2(N_t - 1)/3 + 1$ -small angle- and $N_L = (N_t - 1)/3 + 1$-large angle-) under the effect of different values of puling forces.

The comparison between star shaped and linear polymers is shown in Figure 8. Note that for small angles ($\theta = 5°$) there is an excellent agreement between the linear chain and the star with this deeply asymmetric distribution of pulling forces. This indicates that a star chain in the low angle limit has similar MFBT as a linear polymer chain and that the third arm has no significant contribution to $\langle \tau \rangle$. This fact, together with the information provided by the histograms of Figure 6 confirms the negligible contribution of the third arm to the rupture process due to the small pulling force acting along this branch.

On the other hand, we compare star with a linear polymer in the large angle limit ($\theta = 85°$). Here we have considered that the linear chain is pulled by twice the force of the pulled star (f) for a meaningful comparison. As a result, it is shown that both systems have very different rupture times for low forces. However, a comparison between the star and a linear chain shows a similar behavior for large magnitudes of the pulling forces.

V. CONCLUSIONS

In this work, we analyzed through MD simulations the process of chain scission of symmetric three-arms star shaped polymers subjected to constant external stretching forces. This polymer architecture is the simplest molecular system that allows to explore effect of branching on the mechanisms of thermo-mechanical degradation and to better understand the failure process of a wide variety of polymer systems. From the results, it is possible to draw the following main conclusions:

- The probability density functions provide a schematic illustration of the rupture process as well as of the mobility of the chain beads. However, it is not possible

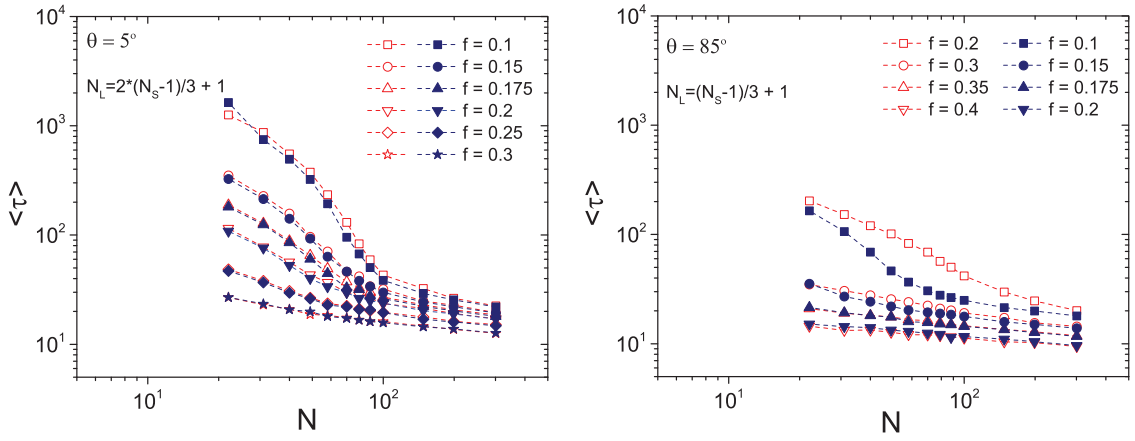

FIG. 8. (Left panel) Comparison of the MFBT between a linear chain of $N_L = 2(N_t - 1)/3 + 1$ beads and a star chain with N_t monomers. (Right panel) Comparison of the MFBT between a linear chain of $N_L = (N_t - 1)/3 + 1$ monomers and a star chain with N_t monomers. Empty symbols denote the linear chain and filled symbols the star chain.

from these distribution maps to know which arm will break more easily since the scission process is governed not only by the local mobility of the beads but also by the distribution of chain stretching along the arms and the inertial effects in the branching point.

- The MFBT dependence on chain length has three different regimes. For large N_t ($N_t \geq 100$), it is possible to propose a power law of the form $\langle\tau\rangle \sim N^{-\beta}$ independent of θ. At intermediate chain lengths, $20 \leq N_t \leq 100$, the MFBT also decreases as N_t increases but in this region $\langle\tau\rangle$ does not follow a power law behavior with N_t. Instead, the MFBT is strongly dependent on θ and any increment in the force shifts the distributions to lower times.
- Regarding the identification of the regions more sensitive to chain scission, the histograms show a negligible contribution of the third arm (pendant arm) in the rupture process for small angles θ. However, for large angles, the situation reverses and the third arm regains prominence and becomes much more probable to break.
- At low angles, the MFBT of linear and star shaped polymer chains behave similarly. In this case, the branching point and the inertial effects associated with the third star arm appears to play no role in the scission process. The comparison among linear and star polymers also holds in the large angle, long chain limits, where the scission events concentrate along the third arm.

ACKNOWLEDGMENTS

N. A. García, M. Febbo, and D. A. Vega acknowledge the financial support of CONICET, Agencia Nacional de Promocion Científica y Tecnológica ANPCyT and Secretaría de Ciencia y Tecnología UNS. A. Milchev acknowledges hospitality during a visit to IFISUR-CONICET.

[1] J. Paturej, A. Milchev, V. G. Rostiashvili, and T. A. Vilgis, EuroPhys. Lett. **94**, 48003 (2011).
[2] J. Paturej, A. Milchev, V. G. Rostiashvili, and T. A. Vilgis, J. Chem. Phys. **134**, 224901 (2011).
[3] M. Rubinstein and R. H. Colby, *Polymer Physics* (Oxford University Press, 2003).
[4] T. C. B. McLeish, Adv. Phys. **51**, 1379–1527 (2002).
[5] D. A. Vega, L. R. Gómez, L. E. Roth, J. A. Ressia, M. A. Villar, and E. M. Vallés, Phys. Rev. Lett. **95**, 166002 (2005).
[6] K. Urayama, K. Yokoyama, and S. Kohjiya, Macromolecules **34**, 4513–4518 (2001).
[7] D. A. Vega and S. T. Milner, J. Polym. Sci.: Part B **45**, 3117–3136 (2007).
[8] S. S. Sheiko, F. C. Sun, A. Randall, D. Shirvanyants, M. Rubinstein, H.-I. Lee, and K. Matyjaszewski, Nature (London) **440**, 191–194 (2006).
[9] N. V. Lebedeva, F. C. Sun, H.-I. Lee, K. Matyjaszewski, and S. S. Sheiko, J. Am. Chem. Soc. **130**, 4228–4229 (2008).
[10] I. Park, S. S. Sheiko, A. Nese, and K. Matyjaszewski, Macromolecules **42**, 1805–1807 (2009).
[11] S. Panyukov, E. B. Zhulina, S. S. Sheiko, G. C. Randall, J. Brock, and M. Rubinstein, J. Chem. Phys. B **113**, 3750–3768 (2009).
[12] S. Panyukov, S. S. Sheiko, and M. Rubinstein, Phys. Rev. Lett. **102**, 148301 (2009).
[13] A. Milchev, J. Paturej, V. G. Rostiashvili, and T. A. Vilgis, Macromolecules **44**, 3981 (2011).
[14] J. Paturej, L. Kuban, A. Milchev, V. G. Rostiashvili, and T. A. Vilgis, Macromol. Symp. **316**, 112–122 (2012).
[15] A. Ghosh, D. I. Dimitrov, V. G. Rostiashvili, A. Milchev, and T. A. Vilgis, J. Chem. Phys. **132**, 204902 (2010).